Measuring brain hemodynamic changes in a songbird: responses to hypercapnia measured with functional MRI and near-infrared spectroscopy

C Vignal[1,2], T Boumans[3], B Montcel[2], S Ramstein[2], M Verhoye[3], J Van Audekerke[3], N Mathevon[1, 4], A Van der Linden[3] and S Mottin[2]

[1]ENES EA 3988, Université Jean Monnet, Saint-Étienne, France

[2]Hubert Curien CNRS UMR 5516, Université Jean Monnet, Saint-Étienne, France

[3]Bio-Imaging Laboratory, University of Antwerp, Antwerp, Belgium

[4]NAMC CNRS UMR 8620, Université Paris XI, Orsay, France

E-mail: mottin@univ-st-etienne.fr

Mottin, S. identifier: http://orcid.org/0000-0002-7088-4353

Short title: Time-resolved NIRS and fMRI for probing hemodynamic changes in a songbird brain.

Key words: Optical Imaging, femtosecond white laser NIRS, brain oximetry, functional Magnetic Resonance Imaging, BOLD signal, zebra finch.

Reference BibTeX

@article{2008_mottin_31,
TITLE = {Measuring brain hemodynamic changes in a songbird: responses to hypercapnia measured with functional MRI and near-infrared spectroscopy},
AUTHOR = { Vignal, Clémentine and Boumans, Tiny and Montcel, Bruno and Ramstein, Stéphane and Verhoye, Marleen and Van Audekerke, Johan and Mathevon, Nicolas and Van Der Linden, Annemie and Mottin, Stéphane },
JOURNAL = {Phys. Med. Biol.},
VOLUME = { 53},
PAGES = { 2457-2470 },
YEAR = {2008},
DOI = {10.1088/0031-9155/53/10/001},
KEYWORDS = {fMRI;BOLD;NIRS;femtosecond laser;hypercapnia;bird;tachymetabolism;Optical Imaging; femtosecond white laser; NIRS; brain oximetry; functional Magnetic Resonance Imaging; zebra finch },
}

Abstract

Songbirds have been evolved into models of choice for the study of the cerebral underpinnings of vocal communication. Nevertheless, there is still a need of *in vivo* methods allowing the real-time monitoring of brain activity. Functional Magnetic Resonance Imaging (fMRI) has been applied in anaesthetized intact songbirds. It relies on blood oxygen level dependent (BOLD) contrast revealing hemodynamic changes. Non-invasive Near-InfraRed Spectroscopy (NIRS) is based on the weak absorption of near-infrared light by biological tissues. Time-resolved femtosecond white laser NIRS is a new probing method using real-time spectral measurements which give access to the local variation of absorbing chromophores like hemoglobins. In this study, we test the efficiency of our time-resolved NIRS device in monitoring physiological hemodynamic brain responses in a songbird, the zebra finch (*Taeniopygia guttata*), using a hypercapnia event (7% inhaled CO_2). The results are compared to those obtained using BOLD fMRI, The NIRS measurements clearly demonstrate that during hypercapnia the local concentration of oxyhemoglobin significantly increases whereas the concentration of deoxyhemoglobin decreases and the total hemoglobin is stable. Our results provide the first correlation in songbirds of the variations in total hemoglobin and oxygen saturation level obtained from NIRS with local BOLD signal variations.

Introduction

Songbirds are well known for their ability to produce and to perceive complex vocal sounds. Consequently, they have been evolved into favourite models for the study of vocal communication and sound processing. The specialized brain structures underlying the capacity of songbirds to recognize and to produce vocal sounds have been investigated mainly with invasive approaches like *post mortem* immunocytochemistry and *in vivo* electrophysiology. To precisely investigate the processes involved in these brain regions, there is a need of a neuro-method that allows real-time monitoring of brain activity of songbirds in a non-invasive manner (Ramstein *et al* 2005).

Recently functional Magnetic Resonance Imaging (fMRI) applied in anaesthetized and mildly sedated intact songbirds was able to reveal brain activity in the auditory system upon hearing conspecific song (Van Meir *et al* 2005, Boumans *et al* 2007, Voss *et al* 2007). Functional MRI that relies on blood oxygen level dependent (BOLD) contrast (Ogawa *et al* 1990) is one of the commonly used techniques for imaging brain activity. During neural activity (Ito *et al* 2001, Ito *et al* 2003), it is expected that an increase of oxygen consumption is followed by a larger fractional increase in cerebral blood flow (CBF) and a lower increase in cerebral blood volume (CBV), resulting in a net decrease in the concentration of deoxygenated hemoglobin. The BOLD fMRI signal is thus a composite signal that is "oxygen-dependent" and remains difficult to be expressed in terms of hemodynamic parameters related to neural activity.

Near-InfraRed Spectroscopy (NIRS) appears as another potential *in vivo* non-invasive method to assess neural activity (Plesnila *et al* 2002, reviewed in Mehta *et al* 2004, *Montcel et al* 2005). Light from the near-infrared spectral window (700-1000 nm) can penetrate deeply into biological tissues according to its weak absorption (Obrig and Villringer 2003, *Ramstein et al* 2005). The spectroscopy of cerebral tissues is thus possible with an intact skull and skin. When the light further propagates through tissue, the attenuation of light intensity depends on

3

the local concentration of absorbing chromophores, like the hemoglobins (Plesnila *et al* 2002, Ramstein *et al* 2005). In this spectral window, the absorption coefficient of tissues relies on the concentration of hemoglobins allowing measurement of variations of oxygen saturation level HbO_2/Hb_{Total} (S_tO_2) and hemoglobin concentration (Hb_{Total}) linked to CBV. Then the light absorption measurements are quantitatively related to oximetry (Obrig and Villringer 2003) which is a robust metabolic marker of cerebral activity (Obrig *et al* 2000). NIRS could thus be envisaged to monitor songbird brain activation. Nevertheless, the exact size and location of the volume of tissue probed by NIRS remains difficult to define because it depends on light scattering by tissues, as well as cellular and subcellular structures (Obrig and Villringer 2003). Contrary to BOLD fMRI, NIRS represents a volumetric probing method allowing poor anatomical resolution. Thus, fMRI and NIRS represent clearly complementary techniques.

As part of our broader effort to develop a non-invasive NIRS method and to improve quantitative measurement of absorbing chromophores into scattering media like biological tissues, we worked on a time-domain based device (Ramstein *et al.* 2005). This time-resolved NIRS involved ultrafast detection of optical signals coupled with a femtosecond white laser and had already allowed to measure optical properties of songbird auditory brain region (Ramstein *et al.* 2005). Using this design, we sought to monitor an evoked brain hemodynamic response which could constitute the basis for our next investigations of songbird brain activity during auditory processing.

In mammals, hypercapnia induces a well-known vasodilatation response that is often used as a model of hemodynamic response (Ito *et al* 2001, Dutka *et al* 2002, Wu *et al* 2002, Ito *et al* 2003, Bluestone *et al* 2004, Martin *et al* 2006). Thus, we used hypercapnia in anesthetized zebra finches (*Taeniopygia guttata*) in order to test the efficiency of our time-resolved NIRS design in monitoring physiological hemodynamic brain responses in a songbird. As a validation, the same experiment was conducted using BOLD fMRI and the results were

4

compared. The use of these two techniques does offer the opportunity to compare the sensitivity of both methods to probe hemodynamic changes in the brain of a songbird, but also makes it possible to correlate in songbirds local variations in Hb_{Total} and S_tO_2 (obtained from NIRS) with local BOLD signal variations (providing overall information on CBF, CBV and S_tO_2) as it has been performed in humans (Kleinschmidt *et al* 1996, Strangman *et al* 2002) and rodents (Siegel *et al* 2003, Martin *et al* 2006).

Material and methods

Animals and general procedure

Adult zebra finches *Taeniopygia guttata* served as subjects for the fMRI and NIRS experiments. Because the fMRI and the NIRS setups were located in distant universities, we were not able to use the same individuals for both experiments. The four birds used in fMRI experiments were obtained from local suppliers in Antwerp (Belgium) and were housed in an aviary with 12L/12D photoperiod, food and water *ad libitum*, and temperature between 23°C and 25°C. The four birds used in NIRS experiments were bred in our aviary (ENES laboratory, Jean Monnet University, Saint-Etienne, France, 12L/12D photoperiod using a full spectrum light with increased blue and red wavelengths fractions, food and water *ad libitum*, temperature between 23°C and 25°C). For fMRI or NIRS measurements, the birds were anaesthetized with 2% isoflurane under spontaneous breathing (isoflurane mixed in fresh air). After a 30 minutes baseline normocapnic period, each bird underwent a challenge of 5 minutes normoxic hypercapnia (600 ml/min 7% CO_2, 21% O_2, 72% N_2, isoflurane mixed at 2%), followed by 5 minutes normocapnia (600 ml/min fresh air, *i.e.* 21% O_2, 79% N_2, isoflurane mixed at 2%) for baseline recovery. Each experiment took less than 1 h. All birds had free access to food and water prior to anaesthesia. Experimental procedures of fMRI measurements were in agreement with the Belgian laws on the "Protection and Welfare of Animals" and had been approved by

the ethical committee of the University of Antwerp. The experimental protocols of NIRS were approved by the Jean Monnet University's animal care committee.

NIRS measurements

Animals preparation

Anaesthetized zebra finches with the head previously plucked (three days before experiments) were fixed in a stereotaxic frame (Stoelting Co., USA, adaptations for birds). The body temperature was kept within a narrow range (39-40°C) by a feedback controlled heating pad. For brain NIRS transillumination, optical fibres were fixed into stereotaxic manipulators (Stoelting Co., USA) and placed directly on the skin. Positions of the input optical fibre F1 providing illumination and the optical fibre F2 collecting transmitted light were chosen in order to probe the auditory regions of the telencephalon (field L, the caudo-medial Nidopallium NCM and the caudo-medial Mesopallium CMM (figure 1)) with the best signal to noise ratio. We have developed a precise and reproducible procedure for placing the optical fibers appropriately on the skin (Ramstein *et al* 2005). The head of the bird is turned until the beak (rostral extremity) is perpendicular to the body plane. This position allowed us to define a stereotaxic origin point (0,0,0) defined by the intersection of the vertical plane passing through the interaural line and the sagittal suture (the vena cerebralis dorsocaudalis) (figure 1). The stereotaxic axes are chosen according to this origin point. Previous works using *post-mortem* tissue (Ramstein *et al* 2005) allowed us to define the coordinates of the auditory regions and to choose the positions of the two fibers (F1 and F2) for optimal optical probing in the right hemisphere. These coordinates minimized the absorption of light due to the sagittal venous sinus, the cerebellum, and the higher skull thickness above the caudal part of the cerebellum. The head volume probed by the light depends greatly on this positioning. Numerical simulations based on a steady-state analytical closed-form Green's function (Kienle and Patterson 1997) for a semi-infinite

geometry showed that the distance between the two fibers must be fixed around 5 mm to facilitate wide probing of the auditory regions (Ramstein *et al* 2005). F1 was placed more rostrally on the right hemisphere than F2 (figure 1). The chosen coordinates (in millimetres) were: F1 (2.0, 5.4, -2.7) and F2 (2.0, 0.4, -0.3),.

Determination of the volume probed by the laser light

In order to compare NIRS and fMRI results, a near identical region of interest must be considered. The boundaries of the volume probed by the laser light are calculated in Ramstein *et al* (2005) using the absorption coefficient $\mu a = 0.083$ mm^{-1} and the reduced scattering coefficient $\mu s' = 4.857$ mm^{-1} which were quantified during the baseline normocapnic period. Rough computations based on simple models of light propagation in a homogeneous medium (Kienle and Patterson 1997) showed that 90% of the collected light probed a tissue volume of 50 mm^3. This volume fits in a box with *XYZ* dimensions of 4 mm x 6 mm x 3 mm centered on the two fibers. Comparison with previous work on *post-mortem* tissue (Ramstein *et al* 2005) showed that the tissue volume probed by the light encompasses mainly the auditory regions. The same computations showed that less than 1% of the collected light probed the vena cerebralis dorsocaudalis and that less than 15% has probed the cerebellum. Although better light propagation models are needed, it showed that the chosen fiber coordinates allowed probing the auditory regions non-invasively.

The boundaries of the volume probed by the laser light were projected on the MR images to extract BOLD signal changes in the same region of interest.

Optical setup and frame processing

The optical setup is described in Ramstein *et al* (2005). It was composed of an ultrafast white laser (the light source) and a time-resolved spectrometer (the detection system). The white laser

was a supercontinuum obtained by focusing amplified femtosecond laser pulses into pure water. The pulses (825 nm, 170 fs, 0.5 mJ, 1 kHz) were produced by a Ti:Sa chirped-pulse amplification laser chain (Coherent Vitesse XT and BMI/Thales alpha 1000). The white light continuum (450 nm to 950 nm) was transmitted to an input optical fibre (core diameter 200 μm, numerical aperture 0.4, length 30 cm). Since the time-resolved spectrometer allows detecting low light levels, very low power level (1 mW) was transmitted through the bird's head (Ramstein *et al.* 2005). After propagation through the bird's head, the light was collected by a collecting optical fibre (same model as the input optical fibre) towards the time-resolved spectrometer. This detection system was composed by a polychromator (270M, Spex Jobin-Yvon) dispersing the light to ensure the spectral analysis and a single shot streak camera (Hamamatsu Streakscope C4334) measuring the time of propagation of the photons through tissues with a temporal resolution of 10 ps. Each measure was a frame integrating 33 laser pulses due to the 33 ms CCD integration time of the streak camera. Due to the jitter effect with 33 laser shots, the temporal resolution was then around 18 ps. The spectro-temporal images had a spectral window extending from 668.0 nm to 844.6 nm on 640 pixels and a temporal window of 1.921 ns on 480 pixels. The picosecond resolution of the time-of-flight of photons was used to probe deep tissues (Ramstein *et al* 2005). The time-resolved transmittance (TRT) is the integral of the intensity of the time-resolved signal for a time window excluding early arrived photons (slightly after the maximum of the transmitted pulse). This time window was empirically chosen to optimize the signal to noise ratio, where the signal is the variation of the TRT during the hypercapnia event. This time window was chosen from 0.188 ns to the end of the recorded signal, 1.921 ns. The full spectrum was analyzed by 20 spectral windows.

The 640 pixels TRT variation spectrum was also fitted to the spectra of oxyhemoglobin (HbO_2) and deoxyhemoglobin (Hb) known in mammals (linear least square regression with Matlab 7.1). The 640 simultaneous linear equations were solved by classic linear least square

procedure. This least-square fitting procedure was applied with the best estimate of the HbO_2 and Hb extinction coefficient spectra (http://omlc.ogi.edu/spectra/hemoglobin/index.html). The same procedure was applied to calculate the variations in concentration of HbO_2 and Hb. These concentration variations can be expressed using an absolute scale (µmol) because our time-resolved detection system can measure the mean optical path through the bird's head thanks to the mean arrival time of photons. Indeed thanks to the mean arrival time of photons (<t>) and the speed of light in tissues (v), it is possible to calculate the variation in the absorption coefficient (Δµa in cm^{-1}) with an absolute scale ($\Delta \mu a = \dfrac{\log\left(1 + \dfrac{\Delta TRT}{TRT}\right)}{v\langle t \rangle}$), and then the absolute variations in concentration of HbO_2 and Hb. The same time window used for the calculation of the TRT was used for the calculation of the mean arrival time of photons. Assuming a mean refractive index of n = 1.4 (v = c / n) as known in mammals tissue (Bolin *et al* 1989), the mean optical path length was found to be 56 mm for an inter-fibres distance of 5.5 mm. Results were then filtered to get rid of the high frequency noise (Chebyshev filter, 120 samples time window (2 s)).

Differences between the TRT values were examined as for fMRI data, using an analysis of variance (ANOVA) for repeated measures, with two factors: 1) the time points; 2) the spectral points (repeated-measures ANOVA, p = 0.05, Statistica Software version 6.1). The ANOVA was followed by a Fisher PLSD post-hoc test (p = 0.05).

Functional MRI measurements

Animals preparation

Anaesthetized zebra finches were immobilized in a non-magnetic lab-made head holder that enabled accurate positioning of the animals within the magnet. To maintain optimal and stable

physiological conditions during measurements, body temperature and respiration were continuously monitored. Body temperature was monitored with a cloacal temperature probe (SA-Instruments, Inc., New York, USA) and maintained at 40.3 ± 0.3 °C (mean ± SD) by a cotton jacket and a water-heated pad connected to an adjustable heating pump (Neslab Instruments, ex111, Newington, CT, USA). Respiration rate and amplitude were monitored with a small pneumatic sensor (SA-Instruments, Inc., New York, USA) positioned under the bird.

fMRI setup

MR imaging was performed at 300 MHz on a 7 Tesla horizontal bore NMR microscope (MR Research Systems, MRRS, UK) with an actively shielded gradient-insert (Magnex Scientific Ltd, Oxfordshire, UK) having an inner diameter of 80 mm and a maximum gradient strength of 400 mT/m. A Helmholtz (45 mm) antenna served for transmitting the radio-frequency (RF) pulses and a circular RF surface antenna (15 mm) was used for MR signal reception. Functional imaging was performed in the right hemisphere (from midline to 4 mm lateral) with a T2*-weighted multislice gradient-echo fast low angle shot (GE-FLASH) sequence: TR 320 ms, TE 14 ms, acquisition matrix 128x62, FOV 25 mm, 8 sagittal slices, slice thickness 0.5 mm, temporal resolution 20 s, and spatial resolution 195x195 µm². Sagittal high-resolution imaging was performed at the same position as the acquired functional slices with a T2-weighted spin-echo (SE) sequence: TR 2000 ms, TE 45 ms, acquisition matrix 256x128, FOV 25 mm, 8 sagittal slices, slice thickness 0.5 mm, spatial resolution 98x98 µm² and number of averages 2. To limit the amount of data to store, the MR measurements were subdivided into one normocapnic run (20 minutes) and one hypercapnic run consisting of a 5 minutes of normocapnia, 5 minutes of hypercapnia and 10 minutes of normocapnia rest period. We acquired 60 functional images during the run of 20 minutes.

The boundaries of the volume probed by the laser light in NIRS experiments were applied on the corresponding high-resolution MR images. The resulting brain regions of interest (ROI) were copied on all time point images of the fMRI experiment and for each slice the mean signal intensity and area size of the selected 2D ROI was calculated for the 60 time points. These mean signal intensities were subsequently expressed as percent signal changes relative to the mean signal intensity of the 10 normocapnic time points preceding the 5 minutes hypercapnic period. The percent signal changes for each time point in the entire volume ROI spread over the 8 sagittal slices -in resemblance to the NIRS data- were calculated with a weighted average taking into account the different 2D ROI area sizes in the eight slices. Statistical analysis of these weighted averaged percent signal changes was performed with SPSS (Statistical Package for Social Sciences, release 12.0). Differences in the percent signal changes were statistically analyzed using an analysis of variance (ANOVA) for repeated measures being the time points.

Results

NIRS measurements

Image processing of the four birds gives a mean temporal evolution of the time-resolved transmittance (TRT) in twenty spectral windows (from 668.0 nm to 844.6 nm) (figure 2A). The timing of the CO_2 perturbation corresponding to the normoxic hypercapnia event is indicated in figure 2. At t = 5 min the concentration of CO_2 was increased to 7% and maintained at this level for 5 minutes. At t = 10 min, the concentration was returned to the baseline level of normocapnia. This defines three successive experimental time periods: normocapnia, hypercapnia and rest.

The ANOVA for repeated measures using the 900 TRT values (one point per second and 15 minutes) as dependent factor demonstrates the existence of a significant effect of the

spectral window (p < 0.001, F = 417.8, df = 19, error = 63194), of the time period (p < 0.001, F = 214.1, df = 2, error = 3326) and of the interaction of the spectral window and the time period (p < 0.001, F = 161.6, df = 38, error = 63194). Figure 2B shows the mean temporal evolution of the TRT in three spectral windows. The one-way ANOVA demonstrates a significant effect for time points during hypercapnia in the spectral window 676.8-685.6 nm (figure 2B; p < 0.001, F = 2.68, df = 499, error = 1500).

Figure 2C shows the mean spectrum of the TRT during normocapnia (mean on 300 TRT normalized to one) and during the four last minutes of hypercapnia (240 TRT). From the 1st to the 13th spectral window (668.0-676.8 nm to 774.0-782.8 nm), the TRT increase during hypercapnia is significant (Post-hoc tests of the repeated measures ANOVA: Fisher PLSD, p < 0.001) (figure 2C).

A least-square fitting procedure is applied with the oxyhemoglobin (HbO_2) and deoxyhemoglobin (Hb) extinction coefficient spectra known in mammals. Despite the difference between the *in vivo* optical properties and the HbO_2 and Hb extinction coefficient spectra measured *ex vivo*, figure 2D shows that the TRT variation originates mainly from the variations in concentration of HbO_2 and Hb. The spectrum peak at 760 nm is significantly measured (figure 2D) and the isobestic region around 800 nm is relatively stable despite the increase of noise induced by the laser pump wavelength (825 nm, 170 fs). The differences between fit and experimental spectrum could come from complex tissues optics phenomena. Despite the fact that the results about cytochrome aa oxidation measurement seem unreliable (Plesnila *et al* 2002, Uludag *et al* 2004), we tested the fit with the cytochrome extinction coefficient spectrum without success.

The HbO_2 and Hb concentration variations throughout the successive time periods (5 min normocapnia, 5 min hypercapnia and 5 min rest) were computed the same way in figure 3. Figure 3 shows the almost symmetrical variations of HbO_2 and Hb, with a 4.6 µmol-increase

12

in HbO_2 and a 7.6 μmol-decrease in Hb during hypercapnia. Therefore the total hemoglobin concentration Hb_{Total} ($Hb_{Total} = HbO_2 + Hb$) appears to be nearly constant during the experiment, with only a slight decrease of 3 μmol during hypercapnia. It should be noted that this decrease remains almost stable during the rest period. Consequently these results show an increase in oxygen saturation level HbO_2/Hb_{Total} (StO_2) while Hb_{Total} remains nearly constant through the normoxic hypercapnia event.

Functional MRI measurements

The mean temporal evolution of the percent BOLD signal changes calculated for the four birds is displayed in figure 4A. The timing of the CO_2 perturbation corresponding to hypercapnia is indicated. Repeated measures ANOVA with the percent BOLD signal changes of the four birds as dependent variables demonstrates the existence of a significant effect for time points during hypercapnia ($p < 0.001$, F = 7.365, df = 58, error = 174). Post hoc comparisons show that these significant differences exist between time points of the two experimental time periods, i.e. normocapnia (t = 0 to t = 5 min) and a subset of the hypercapnia images. We can conclude that fMRI allows the detection of a hypercapnia induced increase of blood oxygenation.

To investigate the effect of the lateral position in the brain (restricted to the eight sagittal slices from midline to 4 mm lateral), we calculated for each slice the mean percent BOLD signal change of the 2D ROI acquired during the last three minutes of hypercapnia (during which a plateau was reached). These data are displayed in figure 4B. A one-way ANOVA with these mean percent BOLD signal change as dependent variable and the sagittal slice position as independent factor demonstrates no significant effect on the mean percent BOLD signal change for lateral position in the brain during both normocapnia ($p = 0.085$, F = 2.086, df = 7), and hypercapnia ($p = 0.901$, F = 0.387, df = 7).

13

Discussion

The present study was aimed at testing the capacity of our ultrafast time-resolved NIRS design to monitor hemodynamic changes in the brain of a songbird and comparing BOLD fMRI and time-resolved NIRS within an identical paradigm. To the best of our knowledge, our results provide the first correlation in songbirds of the variations in total hemoglobin (Hb_{Total}) and oxygen saturation level (StO2) obtained from NIRS with local BOLD signal variation measured with fMRI. Our NIRS results clearly demonstrate that StO2 significantly increases whereas Hb_{Total} is nearly constant during hypercapnia. These variations can be related to the BOLD signal increase detected by fMRI. These results provide the basis of the *in vivo* and non-invasive study in songbirds of the activation of auditory brain regions in response to acoustic stimuli.

BOLD fMRI and NIRS signal changes during normoxic hypercapnia in songbirds

Whereas fMRI detected a significant BOLD signal change reflecting an increase of blood oxygenation during the hypercapnia period, the NIRS measurement detected a hypercapnia induced increase of StO2 while the measured Hb_{Total} remained constant.

Previous studies in mammals reported that hypercapnia induces an increase in CBF (Reivich 1964, Duong *et al* 2001) associated with a small rising CBV (Grubb *et al* 1974, Mandeville *et al* 1998, Ito *et al* 2003). Optical tomography (Bluestone *et al* 2004) and fMRI (Lee *et al* 2001, Dutka *et al* 2002, Wu *et al* 2002) have confirmed these results: the hypercapnia-induced CBF increase without change in oxygen consumption causes an increase in S_tO_2 (Dutka *et al* 2002). Because it provides overall information on CBF, CBV and S_tO_2, the fMRI BOLD signal increase measured during the hypercapnia period of our experiment is in accordance with the expected BOLD response. On the contrary, NIRS allows to quantify distinctively deoxyhemoglobin and oxyhemoglobin, then S_tO_2 and Hb_{Total} linked to CBV. Whereas the increase of S_tO_2 in response to hypercapnia measured by NIRS corresponds to the standard oximetric response to a hypercapnic challenge, we measured a nearly constant Hb_{Total}. The

particularities of avian respiratory and cardiovascular systems (Sturkie 1986) imply that circulatory adjustments in response to gas concentration modifications in birds might differ from mammals. Moreover, an altered hematocrit could explain that the rise in overall CBV is not accompanied by a modification of local CBV expressed by Hb_{Total} (Kleinschmidt *et al* 1996). Thus, it remains to be tested whether this absence of Hb_{Total} variation is explained either by some particularities of the bird physiology or by our protocol. Indeed, 7% CO_2 with normoxia could be insufficient to induce a drastic vasodilatation in the songbird brain.

Differential detection sensitivities of fMRI and NIRS methods

One hypothesis to explore is that the hypercapnia-induced Hb_{Total} variation is below the detection sensitivity of our NIRS design as previously mentioned in other NIRS techniques (Rostrup *et al* 2002). The lack of hypercapnic Hb_{Total}-changes may therefore not be incompatible with previous studies: some authors underlined the relative contribution of extracerebral tissue like the skin, the skull and the cerebral spinal fluid (CSF) to the NIRS signal (Montcel *et al* 2005) which could be a source of less CO_2-reactivity. In our experimental design, we used the time-resolution of NIRS in order to probe deep cerebral tissues and to get the lowest effect from extracerebral tissue. To raise more precisely that question, NIRS should be compared with other methods allowing to assess CBV in birds like MRI using contrast agents (Mandeville *et al* 1998) or ultrasound contrast densitometry (Klaessens *et al* 2005). Moreover, it has been suggested that using a broad range of wavelenghts would be good for a reliable hemoglobin NIRS measurement (Strangman *et al* 2002, Ramstein *et al* 2005). Our NIRS design using a broadband white laser source would allow such spectral investigations.

The chemometric analysis (by linear least-square regression) shows that the variation of transmittance originates mainly from the variation of oxygen saturation (figure 2D). In conclusion, according to picosecond time-of-flight and chemometric spectral analysis, it is clear

that the normoxic 7% hypercapnia induces an increase of local S_tO_2 and a control of Hb_{Total} in the zebra finch brain.

The BOLD signal reflects the effect of paramagnetic deoxygenated hemoglobin upon the magnetic field experienced by the protons in the surrounding water molecules in several spaces including the water within the blood vessels and exterior to the blood vessels, while NIRS measures the modifications of absorption linked only to the vascular bed. The relationship between these two physiological processes needs to be further investigated.

fMRI and NIRS as methods for the in vivo investigation of songbird brain

As fMRI has been shown to be able to discriminate auditory induced activation in the songbird brain (Van Meir *et al* 2005, Boumans *et al* 2007, Voss *et al* 2007), further investigations are needed to raise the following question: could NIRS be used as an alternative or a complementary *in vivo* method to probe acoustically induced brain activity in the songbird brain? In the present work, we compared fMRI and time-resolved NIRS using a hypercapnia protocol that evoked hemodynamic changes throughout the brain. Indeed, the lateral position in the brain did not affect the BOLD signal change during hypercapnia. Our data show that in these conditions both methods detected a significant hemodynamic change with a nearly comparable signal to noise ratio. It remains thus to be tested whether our time-resolved NIRS design could allow to detect signals from highly localized brain regions as fMRI does.

Acknowledgments

References

- *Bluestone Y, Stewart M, Lasker J, Abdoulaev G S and Hielscher A H 2004 Three-dimensional optical tomographic brain imaging in small animals: part 1. Hypercapnia and part 2. Unilateral carotid J. Biomed. Opt. **9** 1046-73*
  CrossrefPubMed
- *Bolin F P, Preuss L E, Taylor C and Ference R J 1989 Refractive index of some mammalian tissues using a fiber optic cladding method Appl. Opt. **28** 2297-303*
  CrossrefPubMed
- *Boumans T*, Theunissen F E*, Poirier C and Van der Linden A 2007 Neural representation of spectral and temporal features of song in the auditory forebrain of zebra finches as revealed by functional MRI Eur. J. Neurosci. **26** 2613-26 (*These authors have contributed equally to this work)*
  CrossrefPubMed
- *Boumans T, Vignal C, Smolders A, Sijbers J, Verhoye M, Van Audekerke J, Mathevon N and Van der Linden A 2008 Functional magnetic resonance imaging in zebra finch discerns the neural substrate involved in segregation of conspecific song from background noise J. Neurophysiol. **99** 931-8*
  CrossrefPubMed
- *Duong T Q, Iadecola C and Kim S G 2001 Effect of hyperoxia, hypercapnia and hypoxia on cerebral interstitial oxygen tension and cerebral blood flow Magn. Reson. Med. **45** 61-70*
  CrossrefPubMed
- *Dutka M V, Scanley B E, Does M D and Gore J C 2002 Changes in CBF-BOLD coupling detected by MRI during and after repeated transient hypercapnia in rat Magn. Reson. Med. **48** 262-70*
  CrossrefPubMed
- *Grubb R L J, Raichle M E, Eichling J O and Ter-Pogossian M M 1974 The effects of changes in PaCO2 on cerebral blood volume, blood flow, and vascular mean transit time Stroke **5** 630-9*
  CrossrefPubMed
- *Ito H, Kanno I, Takahashi K, Ibaraki M and Miura S 2003 Changes in human cerebral blood flow and cerebral blood volume during hypercapnia and hypocapnia measured by positron emission tomography J. Cereb. Blood Flow Metab. **23** 665-70*
  CrossrefPubMed
- *Ito H, Takahashi K, Hatakawa J, Kim S G and Kanno I 2001 Changes in human regional cerebral blood flow and cerebral blood volume during visual stimulation measured by positron emission tomography J. Cereb. Blood Flow Metab. **21** 608-12*
  CrossrefPubMed
- *Kienle A and Patterson M S 1997 Improved solutions of the steady state and the time-resolved diffusion equations for reflectance from a semi-infinite turbid medium J. Opt. Soc. Am. A **14** 246-54*
  Crossref
- *Klaessens J H, Hopman J C, van Wijk M C, Djien Liemb K and Thijssen J M 2005 Assessment of local changes of cerebral perfusion and blood concentration by near infrared spectroscopy and ultrasound contrast densitometry Brain Dev. **27** 406-14*
  CrossrefPubMed
- *Kleinschmidt A, Obrig H, Requardt M, Merboldt K D, Dirnagl U, Villringer A and Frahm J 1996 Simultaneous recording of cerebral blood oxygenation changes during human brain activation by magnetic resonance J. Cereb. Blood Flow Metab. **16** 817-26*

[CrossrefPubMed](#)

- *Lee S P, Duong T Q, Yang G, Ladecola C and Kim S G 2001 Relative changes of cerebral arterial and venous blood volumes during increased cerebral blood flow: implications for BOLD fMRI Magn. Reson. Med.* **45** *791-800*
[CrossrefPubMed](#)
- *Mandeville J B et al 1998 Dynamic functionnal imaging of relative cerebral blood volume during rat forepaw stimulation Magn. Reson. Med.* **39** *615-24*
[CrossrefPubMed](#)
- *Martin C, Jones M, Martindale J and Mayhew J 2006 Haemodynamic and neural responses to hypercapnia in the awake rat Eur. J. Neurosci.* **24** *2601-10*
[CrossrefPubMed](#)
- *Mehta A D, Jung J C, Flusberg B A and Schnitzer M J 2004 Fiber optic in vivo imaging in the mammalian nervous system Curr. Opin. Neurobiol.* **14** *617-28*
[CrossrefPubMed](#)
- *Montcel B, Chabrier R and Poulet P 2005 Detection of cortical activation using time-resolved diffuse optical methods Appl. Opt.* **44** *1942-7*
[CrossrefPubMed](#)
- *Mottin S 2002 Method and device for differential spectrophotometry of non-clear media by means of spectro-temporal imaging in counting mode. WO/2004/013617 European Patent EP1525452 United States Patent 7265826*
- *Obrig H et al 2000 Near-infrared spectroscopy: does it function in functional activation studies of the adult brain? Int. J. Psychophysiol.* **35** *125-42*
[CrossrefPubMed](#)
- *Obrig H and Villringer A 2003 Beyond the visible-imaging the human brain with light J. Cereb. Blood Flow Metab.* **23** *1-18*
[CrossrefPubMed](#)
- *Ogawa S, Lee T M, Kay A R and Tank D W 1990 Brain magnetic resonance imaging with contrast dependent on blood oxygenation Proc. Natl. Acad. Sci. USA* **87** *9868-72*
[CrossrefPubMed](#)
- *Plesnila N, Putz C, Rinecker M, Wiezorrek J, Schleinkofer L, Goetz A E and Kuebler W M 2002 Measurement of absolute values of hemoglobin oxygenation in the brain of small rodents by near infrared reflection spectrophotometry J. Neurosci. Methods* **114** *107-17*
[CrossrefPubMed](#)
- *Ramstein S, Vignal C, Mathevon N and Mottin S 2005 In-vivo and non-invasive measurement of songbird head's optical properties Appl. Opt.* **44** *6197-204*
[CrossrefPubMed](#)
- *Reivich M 1964 Arterial pCO2 and cerebral hemodynamic Am. J. Physiol.* **206** *25-35*
[PubMed](#)
- *Rostrup E, Law I, Pott F, Ide K and Knudsen G M 2002 Cerebral hemodynamics measured with simultaneous PET and near-infrared spectroscopy in humans Brain Res.* **954** *183-93*
[CrossrefPubMed](#)
- *Siegel A M, Culver J P, Mandeville J B and Boas D A 2003 Temporal comparison of functionnal brain imaging with diffuse optical tomography and fMRI during rat forepaw stimulation Phys. Med. Biol.* **48** *1391-403*
[IOPscience](#)
- *Strangman G, Culver J P, Thompson J H and Boas D A 2002 A quantitative comparison of simultaneous BOLD fMRI and NIRS recordings during functional brain activation Neuroimage* **17** *719-31*
[CrossrefPubMed](#)
- *Sturkie P D 1986 Avian Physiology 4th edn (NewYork: Springer)*

[Crossref](#)

- *Toronov V, Walker S, Gupta R, Choi J H, Gratton E, Hueber D and Webba A 2003 The roles of changes in deoxyhemoglobin concentration and regional cerebral blood volume in the fMRI BOLD signal Neuroimage* **19** *1521-31*
  [CrossrefPubMed](#)
- *Uludag K, Steinbrink J, Kohl-Bareis M, Wenzel R, Villringer A and Obrig H 2004 Cytochrome-c-oxidase redox changes during visual stimulation measured by near-infrared spectroscopy cannot be explained by a mere cross talk artefact Neuroimage* **22** *109-19*
  [CrossrefPubMed](#)
- *Van Meir V et al 2005 Spatiotemporal properties of the BOLD response in the songbirds' auditory circuit during a variety of listening tasks Neuroimage* **25** *1242-55*
  [CrossrefPubMed](#)
- *Voss H U, Tabelow K, Polzehl J, Tchernichovski O, Maul K K, Salgado-Commissariat D, Ballon D and Helekar S A 2007 Functional MRI of the zebra finch brain during song stimulation suggests a lateralized response topography Proc. Natl. Acad. Sci. USA* **104** *10667-72*
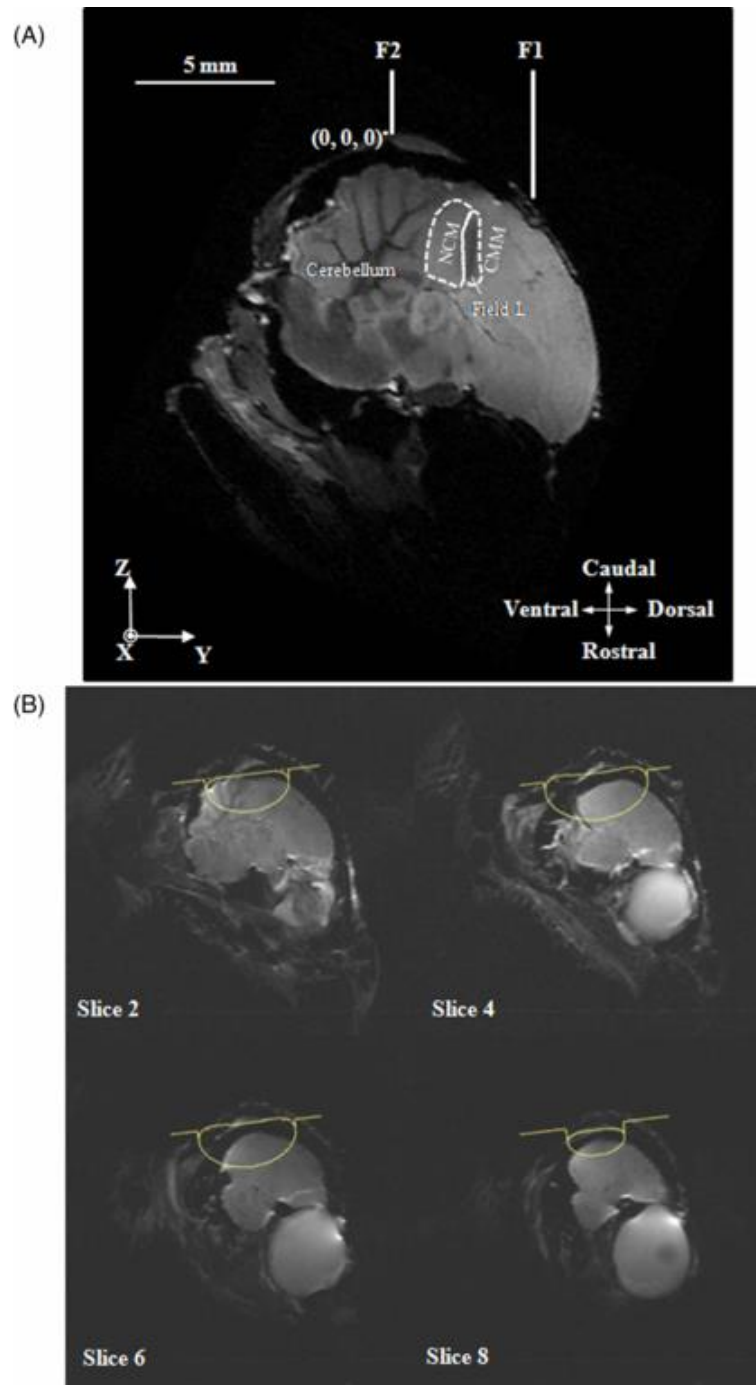 [CrossrefPubMed](#)
- *Wu G, Luo F, Li Z, Zhao X and Li S J 2002 Transient relationships among BOLD, CBV, and CBF changes in rat brain as detected by functional MRI Magn. Reson. Med.* **48** *987-93*
 [CrossrefPubMed](#)

Figure 1

Figure 1. High-resolution magnetic resonance image of the head of a zebra finch (sagittal image in the right hemisphere, 0.8 mm lateral to the sagittal suture). The positions of the regions of interest (Field L, caudo-medial nidopallium NCM and caudo-medial mesopallium CMM) are displayed. The rostro-caudal positions of the input fibre F1 and the collecting fibre F2 of the NIRS setup are shown according to the origin point (0, 0, 0) and the stereotaxic axes (X, Y, Z). Note that F1 and F2 are at 2 mm on the X axis.
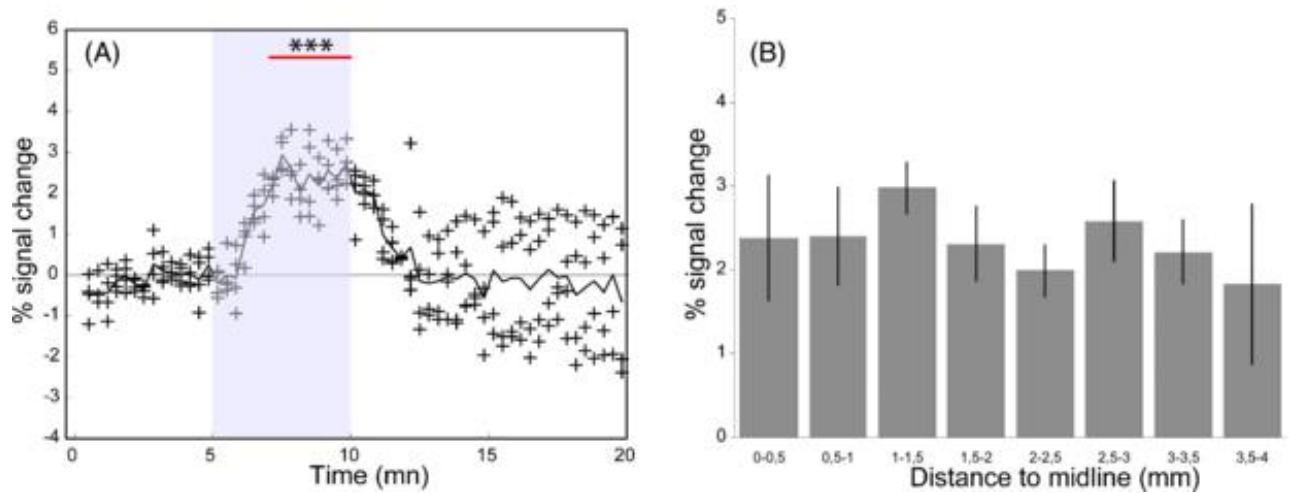
Figure 2
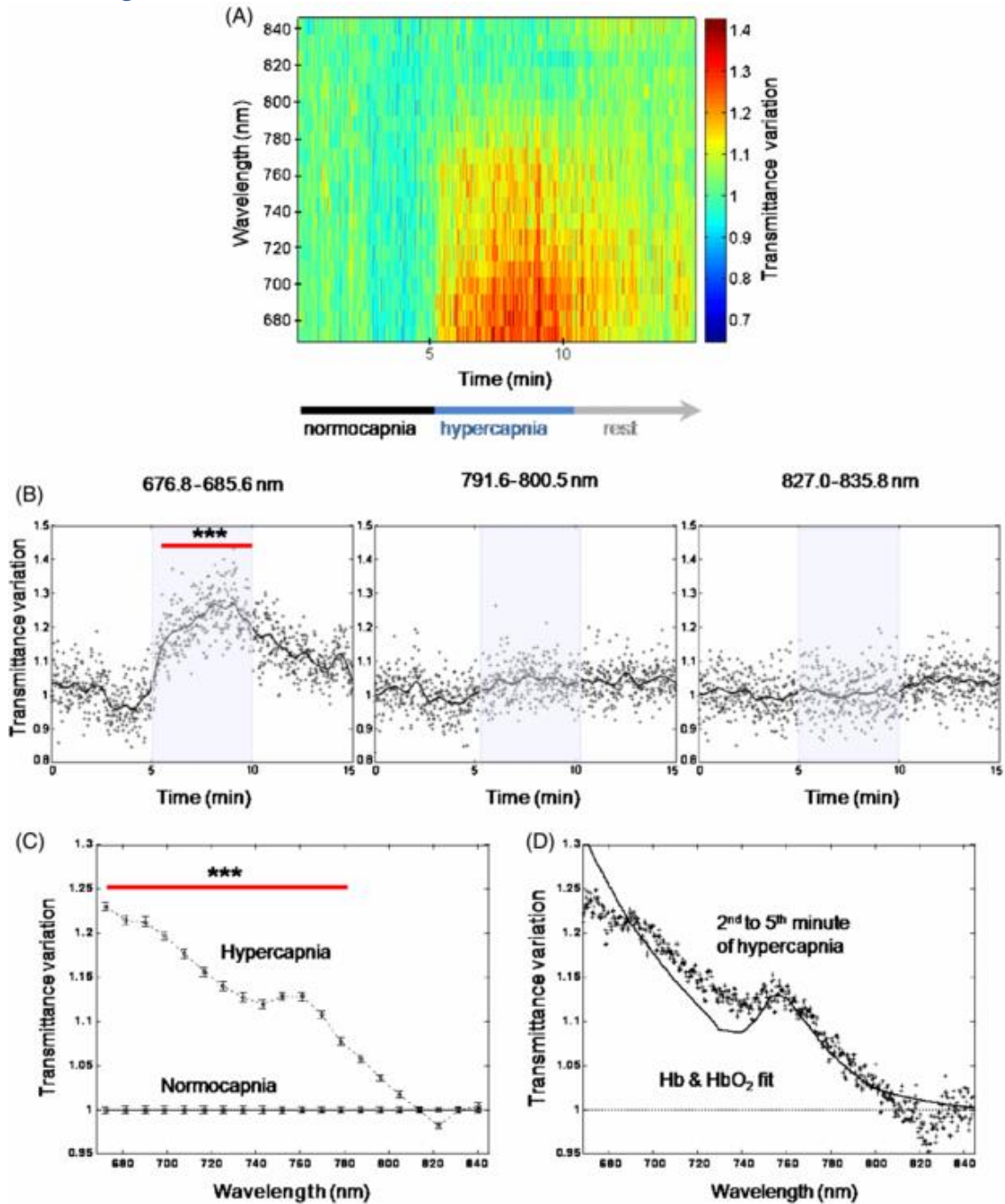
Figure 2. (A) Mean temporal evolution (n = 4 birds) of the time-resolved transmittance (TRT) in 20 spectral windows (Chebyshev time window with a 2s-length). From t = 5 min to t = 10 min the CO_2 concentration was increased to 7%. (B) Mean temporal evolution of the TRT in three spectral windows chosen for univariate analysis (***: $p < 0.001$) (Chebyshev time window with a 60s-length). (C) Mean spectrum of the TRT during normocapnia (mean on 300 TRT normalized to one) and during the four last minutes of hypercapnia (240 TRT). Error bars are standard errors. From the 1st to the 13th spectral windows, the TRT increase during hypercapnia is significant (***: $p < 0.001$). (D) Fit of the TRT spectra variations induced by hypercapnia (four last minutes) to the spectra of oxyhemoglobin (HbO_2) and deoxyhemoglobin (Hb).

21
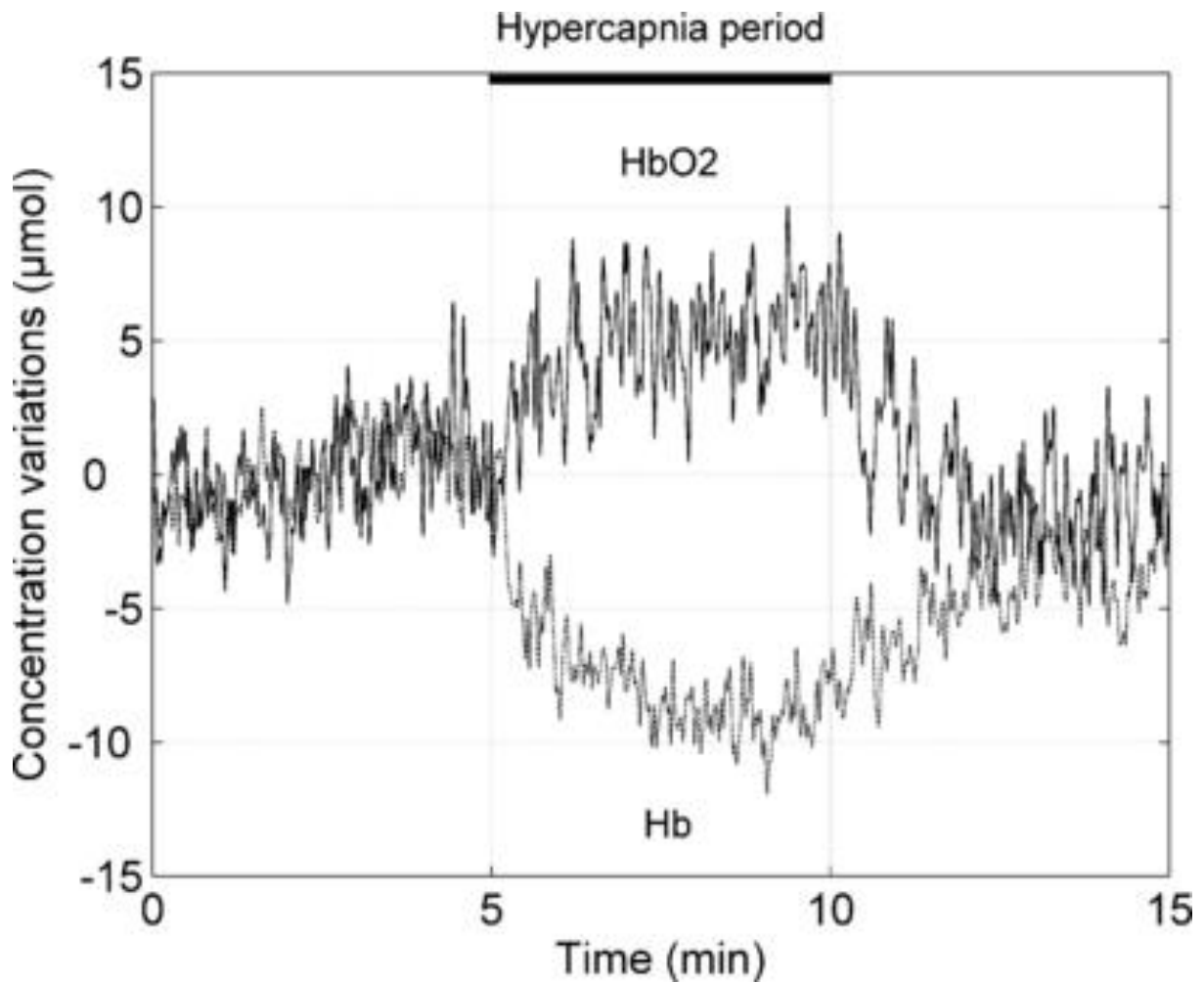
Figure 3

Figure 3. Oxyhemoglobin (HbO$_2$, continuous line) and deoxyhemoglobin (Hb, dashed line) concentrations variations during the normoxic hypercapnia (t = 5 to t = 10 min). Concentrations variations are shown with respect to the normocapnia period (t = 0 to t = 5 min).

Figure 4

Figure 4. (A) Mean temporal evolution of the percent blood oxygen level dependent (BOLD) signal change (n = 4 birds). From t = 5 min to t = 10 min the CO_2 concentration was increased to 7% (***: $p < 0.001$). (B) Mean percent BOLD signal change of the 2D ROI in the eight sagittal slices, averaged over the last three minutes of hypercapnia. ANOVA demonstrates no significant effect of the lateral position in the brain. Error bars are standard errors.